ELSEVIER

Applied Numerical Mathematics 13 (1994) 491–512

APPLIED NUMERICAL MATHEMATICS

Novel stability patterns for the large necking of plates in tension: a numerical study

Pablo V. Negrón-Marrero [a,*], Bárbara L. Santiago-Figueroa [b]

[a] *University of Puerto Rico, Department of Mathematics, Rio Piedras, PR 00931, Puerto Rico*

[b] *Interamerican University, Department of Natural Sciences and Mathematics, Bayamón, PR 00956, Puerto Rico*

Abstract

We study numerically the stability in the energy sense of the necked states of circular plates in tension. We use a finite difference approximation of the displacement boundary value problem giving the necked states. This yields a nonlinear system of equations that depends parametrically on the boundary displacement. To study the bifurcation diagram of this system we use continuation methods and a numerical technique for computing bifurcating branches developed by Rheinboldt. For the linearization of the boundary value problem, we characterize the existence and disposition of eigenvalues on the real line for a large class of physically reasonable constitutive functions that exhibit the standard Poisson ratio effects. For a particular problem we find numerically some stability patterns never observed before.

1. Introduction

The equilibrium equations for the axisymmetric buckling of nonlinearly elastic circular plates under compression, not susceptible to thickness changes, have been studied by Antman [2] and Negrón-Marrero and Antman [20]. These equations represent a geometrically exact description of the deformations of the plate including shear and can be deduced from the three-dimensional theory of elasticity. The corresponding problem with thickness variations has been studied by Negrón-Marrero [19] (no buckling but with a stability analysis of the trivial solution) and Antman [3] (with buckling and nodal preservation for the radial flexure) where global qualitative descriptions of bifurcating branches are given. The constitutive equations in these works satisfy a one-dimensional version of the strong ellipticity condition of three-dimensional

* Corresponding author.

SSDI 0168-9274(93)E0076-E

elasticity. Thus the instabilities found associated with necking are consequences of the nonlinearity of the response rather than of a loss of ellipticity. In most of the works on phase changes (see Ericksen [13], Carr, Gurtin and Slemrod [8,9] among others) these instabilities are due to the nonconvexity of the stored energy function. For some more general plate theories and further references see Naghdi [18].

The corresponding problem for nonlinearly elastic bars in tension has been studied among others by Antman [1], Antman and Carbone [4], and Owen [22]. The work of Owen includes a complete stability analysis of the necked states. In particular, he shows that the only nontrivial stable solutions are the ones with a half-neck or draw representing the first bifurcating branch of solutions.

The main purpose of this work is to study numerically the stability (in the energy sense) of the necked states which result when a circular plate is submitted to some tension. In particular, we want to determine whether or not the result found by Owen [22] for bars holds for the corresponding problem for plates. General stability results for branches of solutions are given by Satinger [25], Crandall and Rabinowitz [12], and Weinberger [28]. All of these results require knowledge of a stable branch of solutions. The results in Maddocks [17] can be used to predict the instability of certain branches without any knowledge of the stability of other branches. This information can be read from the corresponding bifurcation diagram in the so-called displacement–loading graph (cf. Fig. 3).

To work computationally with this problem, we employ a finite difference discretization for its simplicity and stability properties. This enables us to use the package of continuation procedures, called PITCON, developed by Rheinboldt [24]. This program limits itself to trace primary solution curves and only announces when a bifurcation point (of odd algebraic multiplicity) is detected. Since we are precisely interested in determining the stability of the bifurcating branches (which represent necked states of the plate), we use PITCON together with another numerical technique for computing bifurcating branches once they are detected. This other technique is due to Rheinboldt [23] and is specially useful for problems, such as the present case, where the number of variables is large. Having obtained these necked states, we carry out a spectral analysis of the linearization about these states in order to study the stability.

This work is organized as follows. In Section 2 we present the boundary value problem for circular plates in tension which can suffer transverse deformations. In Section 3 we present the corresponding discretized equations. Some of the basics of bifurcation theory and continuation methods are given in Section 4. Rheinboldt [23] describes a numerical technique used to determine a point on a nontrivial branch of solutions near a bifurcation point. This is briefly reviewed in Section 4. In Section 5, we study numerically the stability of the nontrivial solutions of the boundary value problem. The existence and characterization of the disposition of eigenvalues for the linearized problem is a nontrivial problem and represented a source of difficulty in our analysis. This is due to the nonlinear interactions between radial and transversal forces embodied in the characteristic equation (2.16). Despite this, in Section 6, we are able to characterize a large class of physically reasonable constitutive functions that exhibit the standard Poisson ratio effects and to establish the existence of an infinite number of eigenvalues for the corresponding linearized problem. We present some numerical results and further developments in Section 7.

2. The governing equations

Consider a homogeneous nonlinearly elastic circular plate of radius 1, which is subjected to an axisymmetric deformation which is a pure compression or expansion, that is, no bending or shear.

Let $\rho(s)$ be the radius in the deformed configuration of the cylindrical cross-section of radius s in the reference configuration. Similarly, $\omega(s)$ will denote the ratio of the height in the deformed configuration to the height in the reference configuration. Thus the cylindrical cross-section of radius s and height $2h$ in the reference configuration will have radius $\rho(s)$ and height $2h\omega(s)$ in the deformed configuration.

The strains for this problem are

$$\begin{aligned} w(s) &= (\omega(s), \eta(s), \tau(s), \nu(s)) \\ &= (\omega(s), \omega'(s), \rho(s)/s, \rho'(s)), \end{aligned} \tag{2.1}$$

where the "prime" denotes differentiation with respect to "s". Here $\tau(s)$ represents the elongation of a circumferential fiber, $\nu(s)$ the elongation of a radial fiber, and $\eta(s)$ accounts for thickness variations of a mid-cross-section of the plate.

The requirement that an infinitesimal positive volume is not reduced to zero during the deformation leads to the inequalities,

$$\rho(s)/s > 0, \quad \rho'(s) > 0, \quad \omega(s) > 0, \qquad 0 \leqslant s \leqslant 1. \tag{2.2}$$

The stresses which produce each of the strains in (2.1) are

$$\big(\bar{\Omega}(s), \bar{H}(s), \bar{T}(s), \bar{N}(s)\big). \tag{2.3}$$

The momentum balance laws now yield the following systems of equations,

$$\big(s\bar{H}(s)\big)' = s\bar{\Omega}(s), \quad 0 < s < 1, \tag{2.4a}$$

$$\big(s\bar{N}(s)\big)' = \bar{T}(s), \quad 0 < s < 1. \tag{2.4b}$$

The requirement that, during the deformation, the center of the plate remains intact leads to the boundary condition,

$$\rho(0) = 0. \tag{2.5}$$

We will impose a displacement boundary condition at $s = 1$,

$$\rho(1) = \theta, \quad \theta > 0, \tag{2.6}$$

which simply means that in the deformed configuration the outer radius of the plate is θ.

For $\omega(s)$, we have the following boundary conditions,

$$s\bar{H}(s)\,|_{s=0+} = 0, \tag{2.7a}$$

$$\bar{H}(1) = 0. \tag{2.7b}$$

(These follow from an appropriate variational formulation of our problem (see Section 5).)

The material of the plate is *homogeneously elastic*; hence, there exist thrice continuously differentiable functions Ω, H, T, $N:(0,\infty)\times\mathbb{R}\times(0,\infty)^2\to\mathbb{R}$, such that

$$\overline{\Omega}(s)=\Omega(w(s))=\Omega(\omega(s),\ \omega'(s),\ \rho(s)/s,\ \rho'(s)), \tag{2.8}$$

etc.

The strong ellipticity condition of three-dimensional elasticity implies that the constitutive functions $\Omega(\omega,\eta,\tau,\nu)$, etc., satisfy

$$\begin{pmatrix} H_\eta & H_\nu \\ N_\eta & N_\nu \end{pmatrix} \text{ is positive-definite,} \tag{2.9a}$$

$$T_\tau > 0, \tag{2.9b}$$

$$\Omega_\omega > 0, \tag{2.9c}$$

for τ, ν, $\omega>0$ and $\eta\in\mathbb{R}$.

Further we impose the monotonicity condition

$$\begin{pmatrix} N_\nu & N_\tau \\ T_\nu & T_\tau \end{pmatrix} \text{ is positive-definite,} \tag{2.10}$$

where the arguments of the functions are $(\omega, 0, \tau, \nu)$. This condition guarantees that the solutions to our displacement boundary value problem with $\omega'=0$ are unique (see [19]).

Some additional physically reasonable conditions which we require are

$$\Omega,\ T,\ N \text{ even in } \eta, \tag{2.11a}$$

$$H \text{ odd in } \eta. \tag{2.11b}$$

The condition that the material of the plate is isotropic implies that

$$N(\omega,0,\tau,\nu)=T(\omega,0,\nu,\tau), \tag{2.12a}$$

$$\Omega(\omega,0,\tau,\nu)=\Omega(\omega,0,\nu,\tau). \tag{2.12b}$$

We finally impose the growth conditions,

$$\begin{aligned} &N\to\infty && \text{as } \nu\to\infty,\\ &N\to-\infty && \text{as } \nu\to 0^+, \end{aligned} \tag{2.13a}$$

$$\begin{aligned} &T\to\infty && \text{as } \tau\to\infty,\\ &T\to-\infty && \text{as } \tau\to 0^+, \end{aligned} \tag{2.13b}$$

$$H\to\pm\infty \quad \text{as } \eta\to\pm\infty, \tag{2.13c}$$

$$\begin{aligned} &\Omega\to\infty && \text{as } \omega\to\infty,\\ &\Omega\to-\infty && \text{as } \omega\to 0^+. \end{aligned} \tag{2.13d}$$

These limits hold for fixed values of the remaining variables.

Hence, our displacement boundary value problem (BVP) consists of equations (2.4)–(2.7) subject to (2.8)–(2.13).

A solution of the BVP is called *trivial* if $\omega'=0$ and $\rho(s)=\theta s$. With this choice of $\rho(s)$, conditions (2.5) and (2.6) are clearly satisfied. The isotropy condition (2.12a), guarantees that

(2.4b) is satisfied. With these, and using (2.11b), the first equation in (2.4) reduces to

$$\Omega(\omega, 0, \theta, \theta) = 0. \tag{2.14}$$

Conditions (2.9c), (2.13), and the Implicit Function Theorem imply that there exists a C^1 function $\hat{\omega}:(0, \infty) \to (0, \infty)$ such that

$$\Omega(\hat{\omega}(\theta), 0, \theta, \theta) = 0. \tag{2.15}$$

Thus the trivial solution will have $\rho(s) = \theta s$ and $\omega(s) = \hat{\omega}(\theta)$. One can show that condition (2.10) implies that this is the only solution pair with $\omega' = 0$.

The linearization of our BVP about the trivial solution $(\theta s, \hat{\omega}(\theta))$ yields a linear boundary value problem involving the eigenvalue θ. One can show that θ is an eigenvalue of the linearized problem if and only if

$$\frac{N_\omega(\theta)\Omega_\nu(\theta) - N_\nu(\theta)\Omega_\omega(\theta)}{H_\eta(\theta)N_\nu(\theta)} = j_k^2, \tag{2.16}$$

where $N_\omega(\theta) = N_\omega(\hat{\omega}(\theta), 0, \theta, \theta)$, etc., and $\{j_k\}$ are the positive zeros of the Bessel function of the first kind of order 1.

Note that if the function on the left-hand side of (2.16) is negative for all values of θ, then equation (2.16) has no solutions. In this case the linearized problem has to eigenvalues and consequently no bifurcation can occur from the trivial branch $\{(\theta s, \hat{\omega}(\theta)) \mid \theta \in \mathbb{R}\}$.

We summarize the results in [19] concerning the existence of nontrivial solutions (those with $\omega' \neq 0$) for the BVP.

Theorem 2.1. *Let the conditions* (2.9), (2.10), (2.11), (2.12), *and* (2.13) *hold. Let* θ^* *be an eigenvalue of odd algebraic multiplicity of the linearized problem. Then the BVP* (2.4)–(2.7) *subject to* (2.8)–(2.13) *has a connected set of solutions* $C(\theta^*)$ *containing* $(\theta^* s, \hat{\omega}(\theta^*), \theta^*)$ *that satisfies* (2.2) *always and is unbounded in* $(C^1[0, 1])^2 \times \mathbb{R}$, *or contains a point that violates* (2.2), *or contains a point of the form* $(\mu s, \hat{\omega}(\mu), \mu)$, *where* μ *is another eigenvalue of the linearized problem.*

The set $C(\theta^*)$ exists as long as condition (2.2) holds which in turn depends on the growth rates (2.13). When $\theta > 1$, the plate is said to be in *tension*, and these nontrivial solutions can be interpreted as necked states; whereas if $\theta < 1$, the plate is under *compression*, representing barrelled states of the plate.

3. Discretization of the problem

We now describe a finite difference approximation of the BVP of Section 2. Let $\{s_i = ih \mid 0 \leqslant i \leqslant n\}$ be a uniform partition of [0, 1] into n subintervals, with $h = 1/n$. Let $u(s)$ denote a function defined on [0, 1], and u_i an approximation of $u(s_i)$, $0 \leqslant i \leqslant n$.

We will use the notation,

$$\delta u_i = (u_{i+1} - u_i)/h, \tag{3.1a}$$

$$(u/s)_{i+1/2} = (u_{i+1} + u_i)/(s_{i+1} + s_i), \tag{3.1b}$$

$$s_{i+1/2} = (s_{i+1} + s_i)/2, \tag{3.1c}$$

$$G^{i+1/2} = G\big(\omega_{i+1/2},\ \delta\omega_i,\ (\rho/s)_{i+1/2},\ \delta\rho_i\big), \tag{3.1d}$$

for $0 \leqslant i \leqslant n-1$, for any vector $u = (u_0, u_1, \ldots, u_n)$, and for any constitutive functions G, G_τ, $G_v, \ldots$. Note that equations (2.4) and (2.8) are equivalent to

$$s_2 H(w(s_2)) - s_1 H(w(s_1)) = \int_{s_1}^{s_2} t\Omega(w(t))\,\mathrm{d}t, \tag{3.2a}$$

$$s_2 N(w(s_2)) - s_1 N(w(s_1)) = \int_{s_1}^{s_2} T(w(t))\,\mathrm{d}t, \tag{3.2b}$$

for any s_1 and s_2 in $(0, 1)$. Taking $s_1 = s_{i-1/2}$ and $s_2 = s_{i+1/2}$ and using the discretizing operators defined in (3.1) together with the Trapezoidal Rule for approximating integrals, we can discretize (3.2) as

$$\big[s_{i+1/2}H^{i+1/2} - s_{i-1/2}H^{i-1/2}\big] - h\big[s_{i+1/2}\Omega^{i+1/2} + s_{i-1/2}\Omega^{i-1/2}\big]/2 = 0, \tag{3.3a}$$

$$\big[s_{i+1/2}N^{i+1/2} - s_{i-1/2}N^{i-1/2}\big] - h\big[T^{i+1/2} + T^{i-1/2}\big]/2 = 0, \tag{3.3b}$$

for $1 \leqslant i \leqslant n-1$.

The boundary conditions (2.5) and (2.6) are discretized as

$$\rho_0 = 0, \qquad \rho_n = \theta. \tag{3.4}$$

Now taking $s_1 = 0$ and $s_2 = s_{1/2}$ in (3.2a), using the discretizing operators defined in (3.1), together with the right endpoint rule for approximating integrals, we can approximate (2.7a) by

$$s_{1/2}H^{1/2} - hs_{1/2}\Omega^{1/2}/2 = 0. \tag{3.5a}$$

Similarly one can discretize (2.7b) by

$$-\big[s_{n-1/2}H^{n-1/2} + hs_{n-1/2}\Omega^{n-1/2}/2\big] = 0. \tag{3.5b}$$

Our discretized boundary value problem (DBVP) consists of (3.3), (3.4), and (3.5). Thus studying the solutions of the discretized problem, we can get some idea of how the solutions of the BVP of Section 2 behave. The question of how well the solutions of the DBVP approximate those of the BVP shall be pursued elsewhere.

Note that the DBVP defines a mapping $F: D \subset \mathbb{R}^{2n+1} \to \mathbb{R}^{2n}$ where

$$D = \big\{(\omega_0, \omega_1, \ldots, \omega_n, \rho_1, \rho_2, \ldots, \rho_n) \in \mathbb{R}^{2n+1} \mid \omega_i,\ \rho_i > 0 \text{ for all } i,\ \rho_i < \rho_{i+1},\ 1 \leqslant i \leqslant n-1,\ \rho_n = \theta\big\}, \tag{3.6}$$

and F_0 and F_n are defined respectively by (3.5a) and (3.5b), F_i is given by the left-hand side of (3.3a) for $1 \leqslant i \leqslant n-1$ and, for $n+1 \leqslant i \leqslant 2n-1$, F_i is given by the left-hand side of (3.3b).

4. Continuation methods and bifurcation points

The discretized problem (3.3)–(3.5) has the general form

$$F(x, \theta) = 0, \tag{4.1}$$

where $F : D \subset \mathbb{R}^{m+1} \to \mathbb{R}^m$, $x = (x_1, x_2, \ldots, x_m)$, $m = 2n$, and $\theta \in \mathbb{R}$. The function F is called *regular* if its Jacobian matrix, $DF(x, \theta)$ is of full rank for all (x, θ) belonging to

$$S = \{(x, \theta) \mid F(x, \theta) = 0\}. \tag{4.2}$$

Under this condition it can be shown (see [24]) that S consists of continuously differentiable curves that do not intersect. If $(x(t), \theta(t))$ is such a curve passing through the point (x_0, θ_0), then differentiating (4.1) with respect to "t" we obtain the initial value problem:

$$\begin{aligned} &DF(x(t), \theta(t)) \cdot (x'(t), \theta'(t)) = 0, \\ &(x(t_0), \theta(t_0)) = (x_0, \theta_0), \end{aligned} \tag{4.3}$$

where $x'(t) = \mathrm{d}x/\mathrm{d}t$, etc. Most continuation method packages solve (4.3), or an extended system, to "predict" the next point on the curve $(x(t), \theta(t))$, and then "correct" this prediction with an iterative process like Newton's method. This is the case for the package PITCON (see [24]) which is the one we used in our computations of Section 7.

When the regularity condition on F fails we can have bifurcations. More specifically, let $D_x F(x_0, \theta_0) \equiv L_0$ be singular. We say that (x_0, θ_0) is a *simple bifurcation point* if

$$\begin{aligned} &N(L_0) = \operatorname{span}\{u\}, \qquad u^{\mathrm{T}}u = 1, \\ &D_\theta F(x_0, \theta_0) \in R(L_0). \end{aligned} \tag{4.4}$$

A theorem of Crandall and Rabinowitz [11] states that under conditions (4.4) and another condition on the second derivatives, there exist two curves $q_i(t) = (x_i(t), \theta_i(t))$, $i = 1, 2$, such that

$$\begin{aligned} &q_i(0) = (x_0, \theta_0), \quad i = 1, 2, \\ &q_1'(0) \neq q_2'(0). \end{aligned} \tag{4.5}$$

In this case, the theorem of Crandall and Rabinowitz also states that there exists $t_0 > 0$, such that

$$x_2(t) = x_1(t) + tu + \mathrm{o}(t), \quad |t| < t_0, \tag{4.6a}$$

$$\theta_2(t) = \theta_0 + \mathrm{o}(t). \tag{4.6b}$$

Let $L(t) = D_x F(q_1(t))$. If (x_0, θ_0) is a simple bifurcation point, then $h(t) = \det(L(t))$ has a simple root at $t = 0$. Thus, to detect a simple bifurcation point, it suffices to verify the sign of $h(t)$.

Normally the continuation method package limits itself to trace the primary solution curve, say $q_1(t)$ in (4.5), and only announces when a bifurcation point is detected. To compute $q_2(t)$ we used a technique due to Rheinboldt [23] which exploits the representation (4.6) of $q_2(t)$. That is, if we are in a neighborhood of a bifurcation point, then we can approximate $x_1(t)$ in (4.6a) by a Taylor polynomial of order two. We use this approximation in (4.6a), and after

dropping the "o(t)" terms, we get an initial approximation to a point on $x_2(t)$. The method then uses this initial guess in a singular chord method iteration that, under certain conditions, converges to a point on $x_2(t)$. The whole process requires just one evaluation of DF and one LU factorization, and is specially useful for problems in which "m" is large, which is the case here where "m" is proportional to the degree of the approximation. For further details on the method we refer to [23].

5. Stability criteria

In this section we will define what is meant for a solution of the BVP of Section 2 to be "stable", or "unstable" in the energy sense and how to determine numerically the stability.

If the material of the plate is *hyperelastic*, then there exists a function $W:(0, \infty) \times \mathbb{R} \times (0, \infty)^2 \to \mathbb{R}$, called the *stored energy function*, such that

$$\Omega = W_\Omega, \qquad H = W_\eta, \qquad T = W_\tau, \qquad N = W_\nu, \tag{5.1}$$

and the *total energy* of the plate is given by

$$I(\omega, \rho) = \int_0^1 sW(\omega(s), \omega'(s), \rho(s)/s, \rho'(s))\, ds. \tag{5.2}$$

We consider the problem of minimizing $I(\omega, \rho)$ over the set

$$A_\theta = \{(\omega, \rho) \in C^1[0, 1]^2 \mid (2.2), (2.5), \text{and } (2.6) \text{ hold}\}, \tag{5.3}$$

for a given $\theta > 0$, where $C^1[0, 1]$ denotes the space of continuous functions on [0, 1] with continuous derivatives on [0, 1].

A necessary condition for $(\omega, \rho) \in A_\theta$ to be a local minimum of I is that $\delta^2 I(\omega, \rho)$, the second variation of I at (ω, ρ), be positive-semidefinite, i.e.,

$$\delta^2 I(\omega, \rho) \cdot (w, v) \geqslant 0, \tag{5.4}$$

for all smooth (w, v) with $v(0) = 0 = v(1)$. A solution of the BVP will be called *stable* if

$$\delta^2 I(\omega, \rho) \cdot (w, v) > 0, \tag{5.5}$$

for all smooth nontrivial (w, v) with $v(0) = 0 = v(1)$. Otherwise, (ω, ρ) will be called *unstable*, i.e., if there exists nontrivial (w, v) such that equation (5.5) is nonpositive. The following result concerning the stability of the trivial solution of Section 2 is proved in [19]:

Theorem 5.1. *Let condition* (5.1) *hold so that the material of the plate is hyperelastic. Hence the trivial solution* $(\theta s, \hat{\omega}(\theta))$, *defined by* (2.15), *is unstable for those values of* θ *for which*

$$\frac{W_{\nu\omega}^2(\theta) - W_{\omega\omega}(\theta) W_{\nu\nu}(\theta)}{W_{\eta\eta}(\theta) W_{\nu\nu}(\theta)} > j_1^2,$$

where $W_{\nu\omega}(\theta) = W_{\nu\omega}(\hat{\omega}(\theta), 0, \theta, \theta)$, *etc.* (*cf.* (2.16)).

The second variation of I at (ω, ρ) acting on (w, v) smooth with $v(0) = 0 = v(1)$ is defined by

$$\delta^2 I(\omega, \rho) \cdot (w, v) = \frac{\mathrm{d}^2}{\mathrm{d}\varepsilon^2} I(\omega + \varepsilon w, \rho + \varepsilon v)\,|_{\varepsilon = 0}. \tag{5.6}$$

Define the 4×4 matrix $M(\omega, \eta, \tau, \nu)$ by

$$M(\omega, \eta, \tau, \nu) = \begin{pmatrix} \Omega_\omega & \Omega_\eta & \Omega_\tau & \Omega_\nu \\ H_\omega & H_\eta & H_\tau & H_\nu \\ T_\omega & T_\eta & T_\tau & T_\nu \\ N_\omega & N_\eta & N_\tau & N_\nu \end{pmatrix}. \tag{5.7}$$

Then with

$$\begin{aligned} x(s) &= (w(s), w'(s), v(s)/s, v'(s))^{\mathrm{T}}, \\ w(s) &= (\omega(s), \omega'(s), \rho(s)/s, \rho'(s)), \end{aligned} \tag{5.8}$$

an elementary but otherwise lengthy computation shows that

$$\delta^2 I(\omega, \rho) \cdot (w, v) = \int_0^1 s x(s)^{\mathrm{T}} M(w(s)) x(s)\, \mathrm{d}s. \tag{5.9}$$

We now study how to check (5.5) numerically. As in Section 3, let $\{s_i = ih \,|\, 0 \leqslant i \leqslant n\}$ be a uniform partition of the interval [0, 1] into n subintervals, with $h = 1/n$, and recall the notation (3.1). We shall also use the notation $M^{i+1/2}$ for the matrix (5.7) with entries $\Omega_\omega^{i+1/2}$, $\Omega_\eta^{i+1/2}$, etc. Hence, applying the midpoint rule on each of the intervals $[s_i, s_{i+1}]$, $i = 0, \ldots, n-1$, and using the discretizations (3.1), we can approximate (5.2) by

$$I_h(\omega_h, \rho_h) = \sum_{i=0}^{n-1} s_{i+1/2} W^{i+1/2}. \tag{5.10}$$

We now consider the minimization of (5.10) over the set (3.6). It is now easy to check that the (negative of the) first variation of (5.10) is given by (3.3), (3.4) and (3.5), and that the second variation is given by

$$\Delta^2 I_h(\omega_h, \rho_h) \cdot (w_h, v_h) = h \sum_{i=0}^{n-1} s_{i+1/2} \big(x_h^{i+1/2}\big)^{\mathrm{T}} M^{i+1/2} x_h^{i+1/2}, \tag{5.11}$$

where $\omega_h, \rho_h, w_h, v_h \in \mathbb{R}^{n+1}$, and

$$x_h^{i+1/2} = \big((w_h)_{i+1/2}, \delta(w_h)_i, (v_h/s)_{i+1/2}, \delta(v_h)_i\big)^{\mathrm{T}}, \tag{5.12}$$

for $i = 0, \ldots, n-1$. Note that for convenience of notation, we choose to number the components of vectors in $\mathbb{R}^{n+1}$ from 0 to n. Alternately, we can obtain (5.11) by directly applying the midpoint rule to (5.9).

We call a solution pair $(\omega_h, \rho_h) \in \mathbb{R}^{n+1} \times \mathbb{R}^{n+1}$ of the DBVP of Section 3, *h-stable* if

$$\Delta^2 I_h(\omega_h, \rho_h) \cdot (w_h, v_h) > 0, \tag{5.13}$$

for all nontrivial

$$(w_h, v_h) \in \mathbb{R}^{n+1} \times \mathbb{R}^{n+1} \quad \text{with } (v_h)_0 = 0 = (v_h)_n. \tag{5.14}$$

If $\Delta^2 I_h(\omega_h, \rho_h)\cdot(w_h, v_h) \leqslant 0$ for some nontrivial (w_h, v_h) satisfying (5.14), then the solution pair (ω_h, ρ_h) is called *h-unstable*.

Under certain conditions, it can be shown that a solution of the BVP is stable if and only if the corresponding solution of the DBVP is h-stable for h sufficiently small. This question will be pursued elsewhere. For the purpose of this work, we shall assume this fact and thus we take (5.13) and (5.14) as our numerical stability criteria.

We now want to relate the conditions (5.13) and (5.14) to the Jacobian matrix DF of Section 3. For any $(\omega_h, \rho_h) \in D$ (cf. (3.6)), we shall denote by $L(\omega_h, \rho_h)$ the $2n \times 2n$ matrix obtained by evaluating the Jacobian matrix of (3.3)–(3.5) at (ω_h, ρ_h) with the $(2n+1)$st column deleted. We now have:

Theorem 5.2. *Let condition* (5.1) *hold. Hence for any* (w_h, v_h) *satisfying* (5.14) *we have that*

$$\Delta^2 I_h(\omega_h, \rho_h)\cdot(w_h, v_h) = -\langle (w_h, v_h),\, L(\omega_h, \rho_h)\cdot(w_h, v_h)\rangle, \tag{5.15}$$

where $\langle\cdot,\cdot\rangle$ *denotes the usual inner product in* $\mathbb{R}^{2n}$. *Thus a solution* (ω_h, ρ_h) *of the DBVP of Section 3 is h-stable if and only if* $L(\omega_h, \rho_h)$ *is negative-definite.*

Proof. Using the definitions of $M^{i+1/2}$ and $x_h^{i+1/2}$, we can write (5.11) as

$$\begin{aligned}
&\Delta^2 I_h(\omega_h, \rho_h)\cdot(w_h, v_h)\\
&\quad = h\sum_{i=0}^{n-1} s_{i+1/2}\Big[\big(\Omega_\omega^{i+1/2}(w_h)_{i+1/2} + \Omega_\eta^{i+1/2}\delta(w_h)_i + \Omega_\tau^{i+1/2}(v_h/s)_{i+1/2}\\
&\qquad\qquad + \Omega_\nu^{i+1/2}\delta(v_h)_i\big)(w_h)_{i+1/2}\\
&\qquad + \big(H_\omega^{i+1/2}(w_h)_{i+1/2} + H_\eta^{i+1/2}\delta(w_h)_i + H_\tau^{i+1/2}(v_h/s)_{i+1/2} + H_\nu^{i+1/2}\delta(v_h)_i\big)\delta(w_h)_i\\
&\qquad + \big(T_\omega^{i+1/2}(w_h)_{i+1/2} + T_\eta^{i+1/2}\delta(w_h)_i + T_\tau^{i+1/2}(v_h/s)_{i+1/2} + T_\nu^{i+1/2}\delta(v_h)_i\big)(v_h/s)_{i+1/2}\\
&\qquad + \big(N_\omega^{i+1/2}(w_h)_{i+1/2} + N_\eta^{i+1/2}\delta(w_h)_i + N_\tau^{i+1/2}(v_h/s)_{i+1/2} + N_\nu^{i+1/2}\delta(v_h)_i\big)\delta(v_h)_i\Big],
\end{aligned} \tag{5.16}$$

Note that this sum consists basically of four terms involving the constitutive functions Ω, H, T, and N. With the aid of (3.1) and (5.14), the first of these terms can be written as

$$\begin{aligned}
&(h/2)\sum_{i=0}^{n}(w_h)_i\Big[\big(\Omega_\omega^{i+1/2}(w_h)_{i+1/2} + \Omega_\eta^{i+1/2}\delta(w_h)_i + \Omega_\tau^{i+1/2}(v_h/s)_{i+1/2} + \Omega_\nu^{i+1/2}\delta(v_h)_i\big)\\
&\qquad + \big(\Omega_\omega^{i-1/2}(w_h)_{i-1/2} + \Omega_\eta^{i-1/2}\delta(w_h)_{i-1} + \Omega_\tau^{i-1/2}(v_h/s)_{i-1/2} + \Omega_\nu^{i-1/2}\delta(v_h)_{i-1}\big)\Big].
\end{aligned}$$

Similarly one can analyze the other terms in (5.16). Combining these results and the definition of $L(\omega_h, \rho_h)$ we get (5.15).

An examination of the matrix $L(\omega_h, \rho_h)$ shows that it is symmetric. Thus from (5.15) and the definition of h-stability, it follows that a solution (ω_h, ρ_h) of the DBVP of Section 3 is h-stable if and only if $L(\omega_h, \rho_h)$ is negative-definite. □

Thus to determine numerically the h-stability of a solution of the DBVP it is enough to study the eigenvalue structure of $L(\omega_h, \rho_h)$, namely, if all the eigenvalues of $L(\omega_h, \rho_h)$ are negative, then (ω_h, ρ_h) is h-stable. On the other hand, if at least one eigenvalue of $L(\omega_h, \rho_h)$ is positive, then (ω_h, ρ_h) is h-unstable. To study the eigenvalue structure of $L(\omega_h, \rho_h)$ we used the computer package EISPACK (see [27]).

6. Constitutive equations

We now introduce some additional hypotheses, called constitutive equations, which serve to distinguish between different types of material behavior. Since different types of materials react in different ways to the same force, these assumptions will enable us to completely determine our problem from the numerical point of view.

Recall that the material of the plate is hyperelastic if (5.1) holds for some stored energy function $W(\omega, \eta, \tau, \nu)$. The functions W that we consider reflect the physically reasonable hypothesis that infinite compressions or expansions of fibers, surface elements, and volume elements within the body require a correspondingly infinite energy. Thus we let

$$\begin{aligned} W(\omega, \eta, \tau, \nu) &= -\frac{A_1}{1-a_1}(\nu\omega)^{1-a_1} + \frac{B_1}{1+b_1}(\nu\omega)^{1+b_1} - \frac{A_2}{1-a_2}(\tau\omega)^{1-a_2} + \frac{B_2}{1+b_2}(\tau\omega)^{1+b_2} \\ &\quad - \frac{A_3}{1-a_3}(\tau\nu\omega)^{1-a_3} + \frac{B_3}{1+b_3}(\tau\nu\omega)^{1+b_3} + \frac{B_4}{1+b_4}\eta^{1+b_4} + \frac{B_5}{1+b_5}(\eta\nu)^{1+b_5} \\ &\quad + \frac{B_6}{1+b_6}(\eta\tau)^{1+b_6}, \end{aligned} \tag{6.1}$$

where the A_j, $j = 1, 2, 3$, B_i and b_i, $i = 1, \ldots, 6$, are nonnegative and the a_i, $i = 1, 2, 3$, are greater than one. Note that (6.1) satisfies the standard Poisson ratio effects. For example, $W \to \infty$ as $\nu \to 0^+$ or $\nu \to \infty$ while the other variables remain fixed, that is, an infinite energy is required to produce an arbitrarily large compression or expansion of a radial fiber.

It follows now from (5.1) and (6.1) that

$$\begin{aligned} \Omega &= \left(-A_1(\nu\omega)^{-a_1} + B_1(\nu\omega)^{b_1}\right)\nu + \left(-A_2(\tau\omega)^{-a_2} + B_2(\tau\omega)^{b_2}\right)\tau \\ &\quad + \left(-A_3(\tau\nu\omega)^{-a_3} + B_3(\tau\nu\omega)^{b_3}\right)\tau\nu, \end{aligned} \tag{6.2a}$$

$$H = B_4\eta^{b_4} + B_5(\eta\nu)^{b_5}\nu + B_6(\eta\tau)^{b_6}\tau, \tag{6.2b}$$

$$T = \left(-A_2(\tau\omega)^{-a_2} + B_2(\tau\omega)^{b_2}\right)\omega + \left(-A_3(\tau\nu\omega)^{-a_3} + B_3(\tau\nu\omega)^{b_3}\right)\nu\omega + B_6(\eta\tau)^{b_6}\eta, \tag{6.2c}$$

$$N = \left(-A_1(\nu\omega)^{-a_1} + B_1(\nu\omega)^{b_1}\right)\omega + \left(-A_3(\tau\nu\omega)^{-a_3} + B_3(\tau\nu\omega)^{b_3}\right)\tau\omega + B_5(\eta\nu)^{b_5}\eta. \tag{6.2d}$$

We now relate (6.1) to the conditions (2.11) and (2.12).

Proposition 6.1. *The function* (6.1) *satisfies the isotropy condition* (2.12) *if*

$$\begin{aligned} A_1 &= A_2, & B_1 &= B_2, \\ a_1 &= a_2, & b_1 &= b_2. \end{aligned} \tag{6.3}$$

In addition, (2.11) *holds if*

$$b_4,\ b_5,\ \text{and } b_6 \text{ are odd.} \tag{6.4}$$

Proof. Upon inspection of (6.2a), (6.2c), and (6.2d), one can easily see that (6.3) implies (2.12). Note also that from (6.2), it follows that Ω is independent of η, N contains η only to the power b_5+1, T contains η only to the power b_6+1, and H contains η to the powers b_4, b_5, and b_6. Thus (2.11) holds if (6.4) holds. □

The parameters A_i, B_i, a_i, and b_i in (6.1) determine completely the material behavior of the plate. Different values of these parameters would determine whether the plate is composed of rubber, wood, etc. We now study the existence of solutions of the equation (2.16) when (5.1) and (6.1) hold.

Theorem 6.2. *Let* (6.3) *hold and assume that* $b_4 = 1$ *and that* $a_i = b_i = a$, $i = 1, 2, 3$, *in* (6.1). *If* $1 < a < 1 + \frac{2}{3}\sqrt{3}$, *then* (2.16) *has an infinite number of solutions* $\{\theta_m\}$ *with* $\theta_m \to \infty$ *as* $m \to \infty$.

Proof. Let $\alpha = \hat{\omega}(\theta)$ be the solution of equation (2.15) (or (2.14)). Then, from (6.2) we get that

$$\begin{aligned} N_\Omega(\theta) &= (a-1)A_1(\theta\alpha)^{-a} + (a+1)B_1(\theta\alpha)^a \\ &\quad + \big((a-1)A_3(\theta^2\alpha)^{-a} + (a+1)B_3(\theta^2\alpha)^a\big)\theta, \end{aligned} \tag{6.5a}$$

$$N_\nu(\theta) = \big(aA_1(\theta\alpha)^{-a-1} + aB_1(\theta\alpha)^{a-1}\big)\alpha^2 + \big(aA_3(\theta^2\alpha)^{-a-1} + aB_3(\theta^2\alpha)^{a-1}\big)(\theta\alpha)^2, \tag{6.5b}$$

$$\Omega_\omega(\theta) = 2\big(aA_1(\theta\alpha)^{-a-1} + aB_1(\theta\alpha)^{a-1}\big)\theta^2 + \big(aA_3(\theta^2\alpha)^{-a-1} + aB_3(\theta^2\alpha)^{a-1}\big)\theta^4. \tag{6.5c}$$

Equation (2.15) can be written as

$$2\big(-A_1(\theta\alpha)^{-a} + B_1(\theta\alpha)^a\big)\theta + \big(-A_3(\theta^2\alpha)^{-a} + B_3(\theta^2\alpha)^a\big)\theta^2 = 0. \tag{6.6}$$

This equation can be solved for α yielding

$$\alpha^{2a} = \theta^{-3a+1}\frac{2A_1\theta^{a-1} + A_3}{2B_1 + B_3\theta^{a+1}}. \tag{6.7}$$

From this expression we get the asymptotic formulas:

$$\begin{aligned} &\alpha \sim (2A_1/B_3)^{1/2a}\theta^{-(3a+1)/2a}, \quad \theta \to \infty, \\ &\alpha \sim (A_3/2B_1)^{1/2a}\theta^{-(3a-1)/2a}, \quad \theta \to 0^+. \end{aligned} \tag{6.8}$$

Combining (6.5) with (6.8) we get that

$$\begin{aligned} N_\omega(\theta) &\sim c_1\theta^{(a+1)/2}, && \theta \to \infty, \\ N_\omega(\theta) &\sim c_2\theta^{(-a+1)/2}, && \theta \to 0^+, \end{aligned} \tag{6.9a}$$

$$\begin{aligned} N_\nu(\theta) &\sim c_3\theta^{(a/2)-2-(1/2a)}, && \theta \to \infty, \\ N_\nu(\theta) &\sim c_4\theta^{-(a/2)-2+(1/2a)}, && \theta \to 0^+, \end{aligned} \tag{6.9b}$$

$$\begin{aligned} \Omega_\omega(\theta) &\sim c_5\theta^{3+(a/2)+(1/2a)}, && \theta \to \infty, \\ \Omega_\omega(\theta) &\sim c_6\theta^{3-(a/2)-(1/2a)}, && \theta \to 0^+, \end{aligned} \tag{6.9c}$$

where

$$\begin{aligned} c_1 &= (a+1)A_1(B_3/2A_1)^{1/2} + aB_3(2A_1/B_3)^{1/2}, \\ c_2 &= (a-1)B_1(A_3/2B_1)^{1/2} + aA_3(2B_1/A_3)^{1/2}, \\ c_3 &= aA_1(2A_1/B_3)^{(1-a)/2a} + aB_3(2A_1/B_3)^{(a+1)/2a}, \\ c_4 &= aB_1(A_3/2B_1)^{(a+1)/2a} + aA_3(A_3/2B_1)^{(1-a)/2a}, \\ c_5 &= 2aA_1(2A_1/B_3)^{-(a+1)/2a} + aB_3(2A_1/B_3)^{(a-1)/2a}, \\ c_6 &= 2aB_1(A_3/2B_1)^{(a-1)/2a} + aA_3(A_3/2B_1)^{-(a+1)/2a}. \end{aligned} \tag{6.10}$$

If we let $Q(\theta)$ denote the function on the left-hand side of (2.16), then we get from (6.9), (6.10), and $b_4 = 1$ that

$$Q(\theta) \sim \frac{-3a^2+6a+1}{2c_3B_4}\theta^{a/2+3+1/2a}, \quad \theta \to \infty, \tag{6.11a}$$

$$Q(\theta) \sim \frac{-3a^2-6a+1}{2c_4B_4}\theta^{3-a/2-1/2a}, \quad \theta \to 0^+. \tag{6.11b}$$

The result of the theorem now follows since the coefficient of the power of θ in (6.11a) is positive provided $1 < a < 1 + \frac{2}{3}\sqrt{3}$. □

7. Numerical results and conclusions

We combined the methods described in Sections 4–6 into a computer program that finds approximate solutions of the system (3.3)–(3.5). The basic parts of this program are as follows:

(a) Given a starting value of θ, we compute the trivial solution corresponding to this θ by solving the equation (2.14) using Newton's method.
(b) Starting from the solution computed in (a), we use the program PITCON to generate the curve of trivial solutions. The sign of the determinant of D_xF is checked to detect possible bifurcation points.

Table 1
Values for coefficients of (6.1)

i	A_i	B_i	a_i	b_i
1	1	1	2	2
2	1	1	2	2
3	1	1	2	2
4	–	10	–	2
5	–	1	–	2
6	–	1	–	2

(c) Once a bifurcation point is detected, that is, a change in the sign of the determinant of $D_x F$, a bisection method is used to reduce the length of the interval in which the bifurcation point lies.
(d) Each bifurcation point localized in (c) is processed with the algorithm described in Section 4 to get a point on the bifurcating branch. Once this point on the new branch is successfully detected, we use PITCON again to continue tracing the bifurcating branch.
(e) On each point of the computed branches, the stability criteria of Section 5 are applied.

We used $n = 64$ in equations (3.3), (3.4), and (3.5) and the values for the coefficients in (6.1) as given in Table 1. All computations were carried in double precision on an IBM RS/6000 and full machine precision was used in PITCON, i.e., the absolute and relative error tests in the routine used the machine epsilon.

The numerical results indicate that the trivial branch is stable up to the first bifurcation point ($\theta = 6.1934$ approximately) after which it becomes unstable. This result is in agreement with Theorem 5.1. We computed part of the first three nontrivial bifurcating branches. In Fig. 1

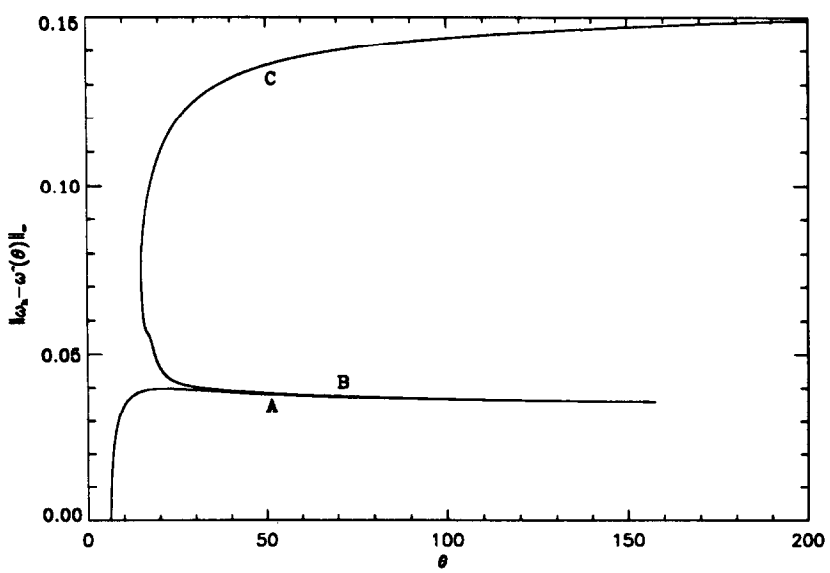

Fig. 1. First branch of nontrivial solutions bifurcating from $\theta = 6.1934$ approximately.

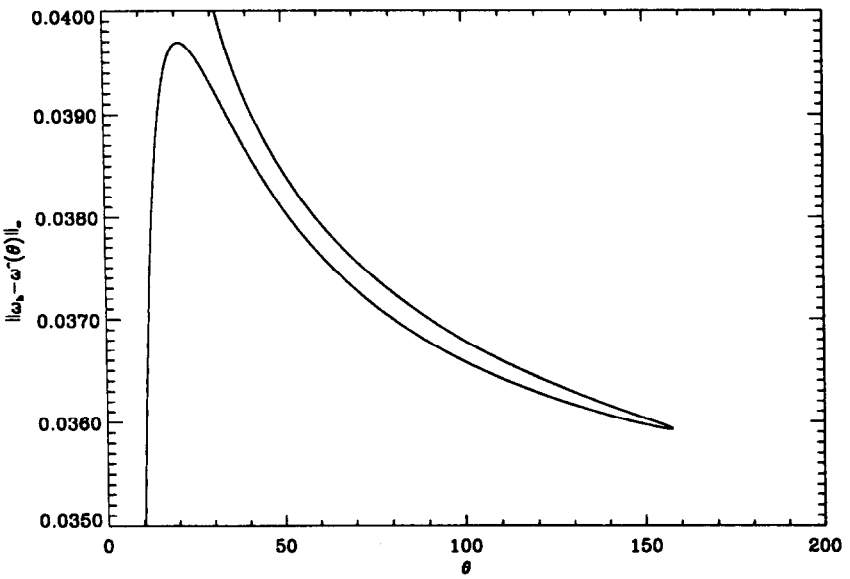

Fig. 2. A blow-up of the section of the first branch corresponding to the turning point opening to the left.

we show part of the first branch. The vertical axis in this figure is a measure of the nonuniformity of the deformation in terms of the thickness, i.e.,

$$\| \omega_h - \hat{\omega}(\theta) \|_\infty = \max_{0 \leqslant i \leqslant n} |(\omega_h)_i - \hat{\omega}(\theta)|.$$

There are two turning points at approximately $\theta = 157.55$ and $\theta = 14.88$. The sections of the branch labeled A, B, and C are stable, unstable, and stable respectively in the sense of Section 5. We show in Fig. 2 a blow-up of the neighborhood of the turning point at $\theta = 157.55$ which shows more details of this section of the branch. In Fig. 3 we show the displacement–load diagram for the first branch. Here the loading Λ_h is defined by

$$\Lambda_h = N((\omega_h)_n, 0, \theta, r_h),$$

where we use the $O(h^2)$ approximation of $\rho'(1)$ given by

$$r_h = \frac{1}{2h}(3(\rho_h)_n - 4(\rho_h)_{n-1} + (\rho_h)_{n-2}).$$

The sections labeled A, B, and C correspond to those labeled similarly in Fig. 1. Note that the stability changes in this diagram are exactly at the horizontal folds of the curve (see [17]). One can observe also that as we traverse this curve in the direction of increasing displacement, the loading decreases except for the section of the curve between ($\Lambda_h = 1.291$, $\theta = 14.88$) and ($\Lambda_h = 1.794$, $\theta = 45.84$) where it increases. This lack of monotonicity in the loading response is characteristic of "plastic" behavior and in problems of phase transitions (see, e.g., [8,9,13]). Note however that the function N in (6.2d) is monotone in ν. Finally in Fig. 4 we show an energy–displacement diagram for the first branch. The section labeled C on the first branch has the lowest energy except for a section to the left of $\theta = 20$. Note that the turning points in

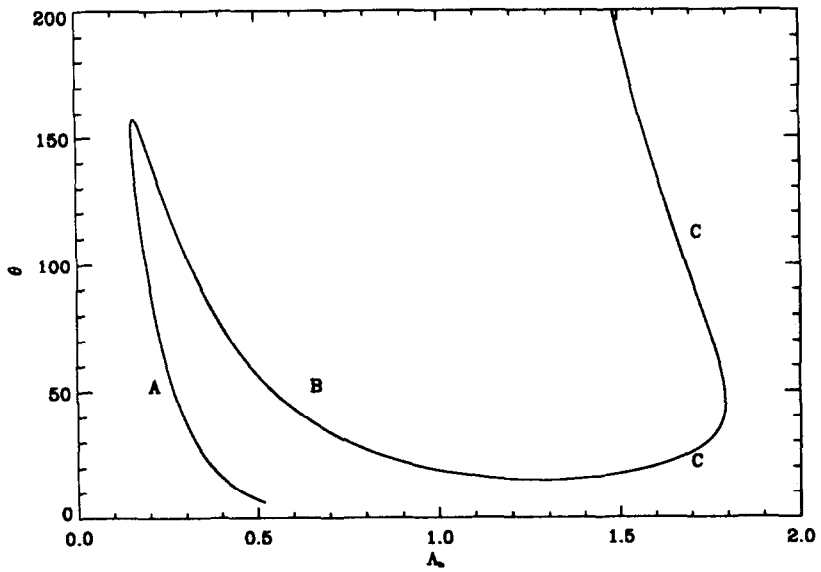

Fig. 3. Displacement–load diagram for the first branch.

this diagram (which coincide with those of Fig. 1), which correspond to stability changes, are "cusps" as predicted by the theory.

The qualitative behavior of the second branch is more complicated than that of the first and is shown in Fig. 5. The branch is unstable at the bifurcation point $\theta = 7.8$ approximately, and undergoes a stability change in the region shown separately in Fig. 6. The sections of the

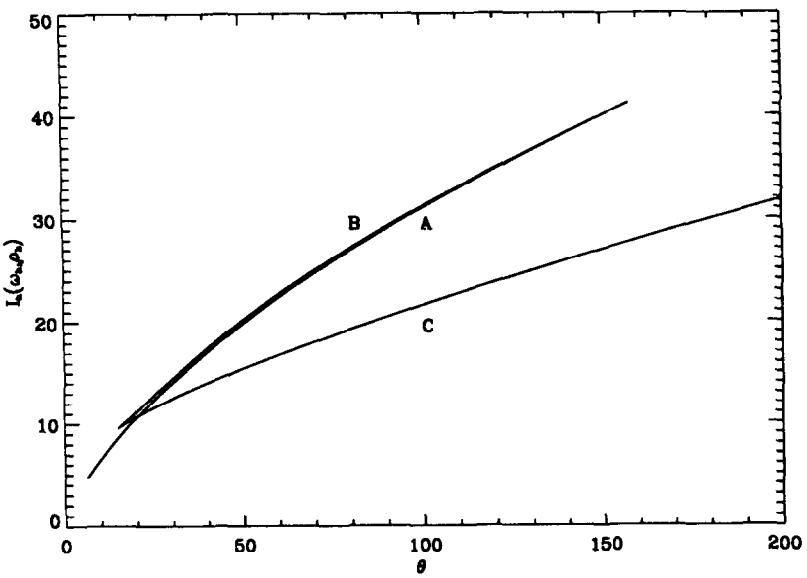

Fig. 4. Energy–displacement diagram for the first branch.

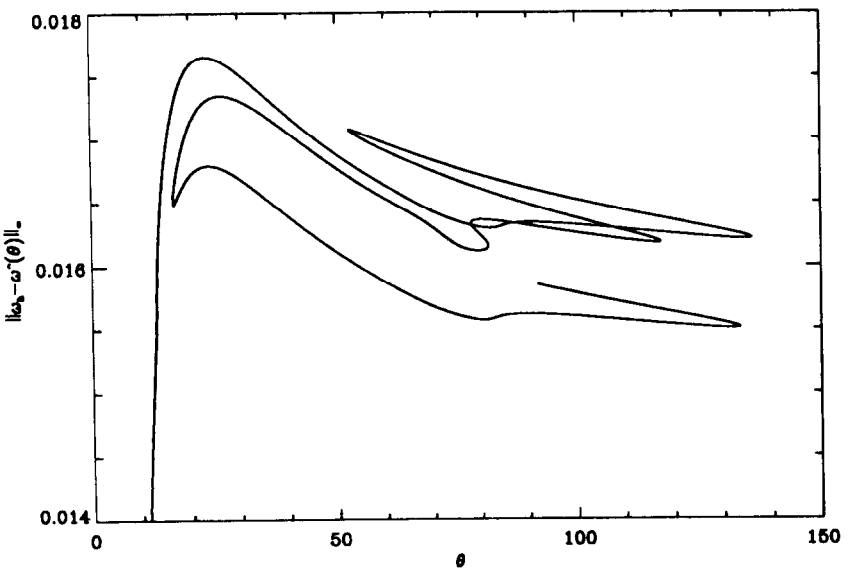

Fig. 5. Second branch of nontrivial solutions bifurcating from $\theta = 7.8645$ approximately.

branch labeled A, B, and C are stable, unstable, and stable respectively. The fact that there are stable solutions on a branch representing multiple necked states and that there are unstable solutions on the first branch is completely different to the corresponding result for bars in tension found by Owen [22].

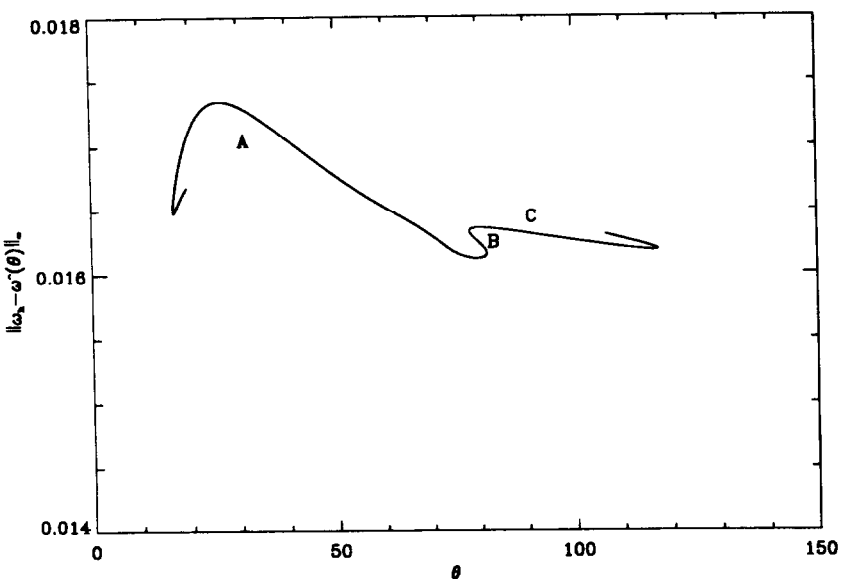

Fig. 6. Stable (A, C) and unstable (B) sections of the second branch.

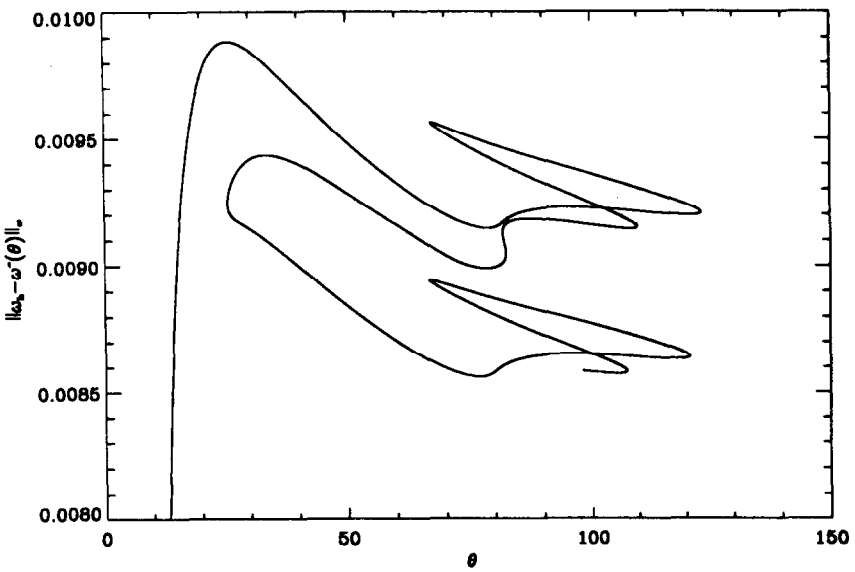

Fig. 7. Third branch of nontrivial solutions bifurcating from $\theta = 9.2203$ approximately.

In Fig. 7 we show part of the third branch corresponding to solutions of (3.3), (3.4), and (3.5) with two full "necks". Again the qualitative behavior is very complicated, however no stable solutions were found in this branch. Figs. 8–10 show mid-cross-sections of solutions from each branch corresponding to $\theta = 20$. These pictures include the information of both ω_h and ρ_h. The dotted-line curve represents the corresponding trivial solution. The height of the original plate has been normalized to one.

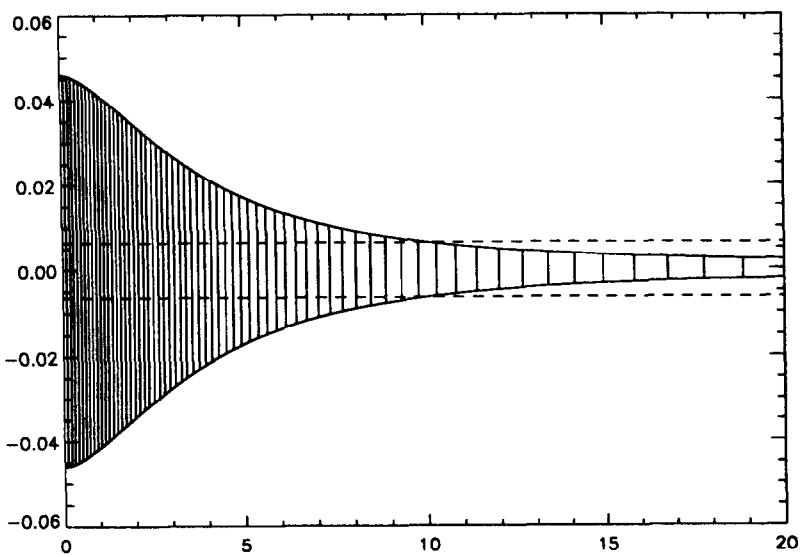

Fig. 8. Mid-cross-section of the plate corresponding to a stable solution on the first branch and $\theta = 20$.

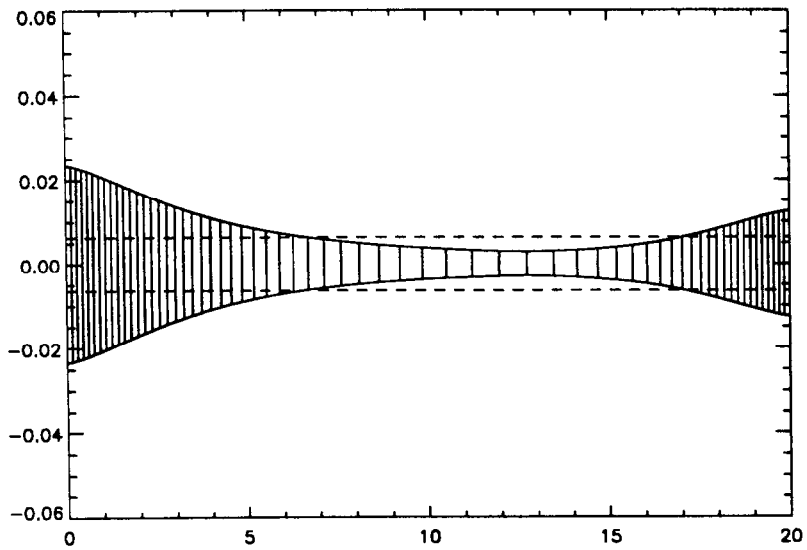

Fig. 9. Mid-cross-section of the plate corresponding to a stable solution on the second branch and $\theta = 20$.

Finally to test the convergence of the discretization of Section 3, we computed solutions on the first branch for $\theta = 20$ and for $n = 4, 8, \ldots, 64$. We used the solution corresponding to $n = 128$ as the exact discretized solution for the purpose of estimating the errors. We use the notation

$$e(\omega_n) = \| \omega_n - \omega_{128} \|_\infty,$$

where ω_n stands for the solution ω_h corresponding to $h = 1/n$. (Here we understand that in

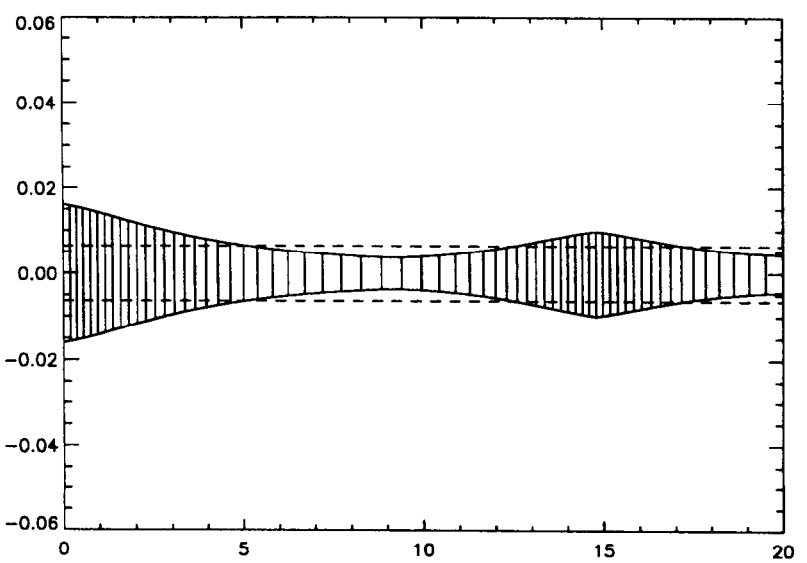

Fig. 10. Mid-cross-section of the plate corresponding to an unstable solution on the third branch and $\theta = 20$.

Table 2
Computed solution for first branch; $\theta = 20$

n	$e(\omega_n)$	$e(\omega_n)/e(\omega_{2n})$	$e(\rho_n)$	$e(\rho_n)/e(\rho_{2n})$
4	0.603516E−02	–	0.816343E+00	–
8	0.299702E−02	0.201372E+01	0.138659E+00	0.588739E+01
16	0.111665E−02	0.268394E+01	0.271721E−01	0.510301E+01
32	0.360440E−03	0.309801E+01	0.577927E−02	0.470165E+01
64	0.879578E−04	0.409788E+01	0.148201E−02	0.389961E+01

$\omega_n - \omega_{128}$ only the components of ω_{128} corresponding to those of ω_n are used in the computation.) The results, shown in Table 2, show an approximate rate of convergence of $O(h^2)$. The nonlinearities implicit in (2.8), the restrictions (2.2), and the singular behaviors embodied in (2.13) make the full analysis of convergence of the method of Section 3 a nontrivial task. A simpler version of this problem, but still exhibiting the nonlinear and singular behaviors, is analyzed in [21] where the discretization of the corresponding model for the deformations of the plate without necking (consisting basically of just the second equation in (2.4)) is shown to have $O(h^2)$ convergence rate. The results in [5–7] should be helpful in the full analysis of the discretization of Section 3. This approach will be pursued elsewhere.

Our results show that the nonlinear plate theory considered here is richer than the corresponding rod theory studied by Owen [22] and consequently it can be used to describe phenomena that are usually explained or associated with plastic behavior. There is however one important point to bear in mind when comparing both results. Suppose that instead of a displacement boundary value problem, we pose the problem of Section 2 as a dead-load boundary value problem, that is, we specify $N(1)$ instead of $\rho(1)$ (cf. (2.6)). Hence the corresponding variational formulation of the problem would correspond to an unconstrained problem of the calculus of variations and the problem of Section 5 would be the constrained problem corresponding to the constraint (2.6). The set of equilibrium points for both problems coincides. For the particular problem we treated, the first three branches of such equilibria are given by Figs. 1, 5, and 7. For the unconstrained problem, the stability criterion is given by (5.5) but only with the condition $v(0) = 0$. The stability criterion that we used in Section 5 is thus equivalent to the second variation of the unconstrained problem be positive-definite on the tangent space defined by the constraint. This reduces to (5.5) with $v(0) = 0 = v(1)$. Thus, an equilibrium point could be stable for the constrained problem but unstable for the unconstrained version. In fact, the first branch depicted in Figs. 1 and 3 was found to be unstable for the unconstrained problem. Thus it could be the case that the stability results in Owen [22], which are for the dead-load problem, are different when the corresponding displacement problem is analyzed.

A simple perturbation analysis about, say, the first bifurcation point shows that in general we have a pitchfork bifurcation at such point. (This is true for the general problem stated in Section 2.) We computed the other part of the pitchfork corresponding to the branch in Fig. 1 and found that it corresponds to an unsymmetric pitchfork of the type shown schematically in Fig. 11. (The dashed section of the curve represents unstable equilibria.) The equilibria on the other part of the pitchfork have the same qualitative shape as in Fig. 8 but thinner on the center and fatter on the boundary.

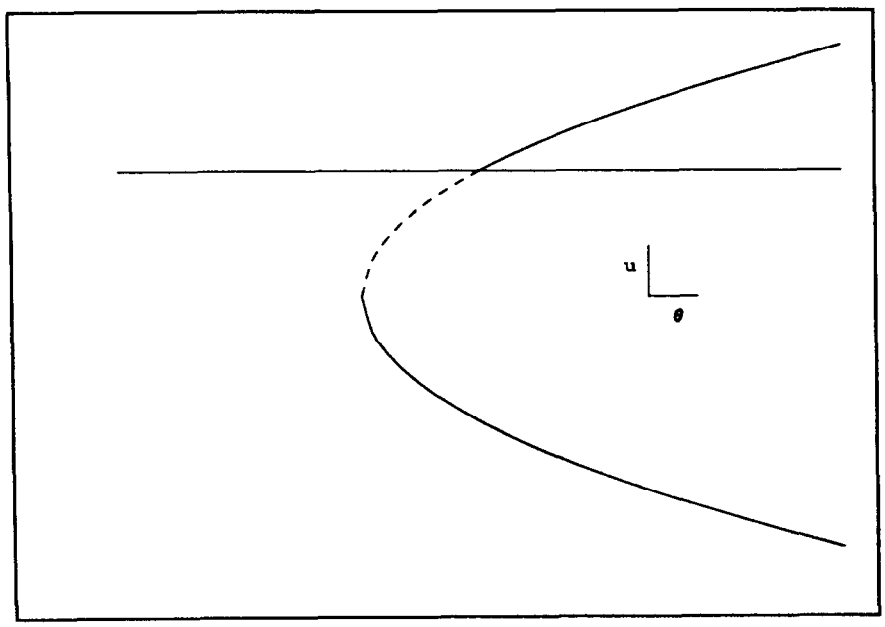

Fig. 11. Schematic representation of the unsymmetric pitchfork corresponding to the branch in Fig. 1. The dashed portion of the curve represents unstable equilibria.

The numerics for the particular problem we treated, also indicate that the number of simple interior zeros of $\omega - \hat{\omega}(\theta)$ in [0, 1], inherited from the corresponding eigenfunction, is preserved globally along a given bifurcating branch. This has been shown for a general class of nonlinear boundary value problems for regular ordinary differential equations (ODEs) by Crandall and Rabinowitz [10], for certain systems of ODEs that can be reduced to a scalar equation by Shih and Antman [26] and Negrón-Marrero and Antman [20], for a special class of systems of ODEs with a "weak" coupling by Healey [14], and for scalar quasilinear partial differential equations with symmetries by Healey and Kielhofer [15,16]. We shall pursue this question for our problem elsewhere.

8. Acknowledgements

This work was supported in part by the National Science Foundation under grant number DMS-8722521 and EPSCoR of Puerto Rico (Negrón-Marrero, Santiago-Figueroa), and in part by the Federal Department of Education (Santiago-Figueroa). Some of the computer facilities used are part of the Gauss Laboratory for Mathematical Research, of the Department of Mathematics, UPR, Rio Piedras, Puerto Rico.

9. References

[1] S.S. Antman, Nonuniqueness of equilibrium states of bars in tension, *J. Math. Anal. Appl.* 44 (1973) 333–349.
[2] S.S. Antman, Buckled states of nonlinearly elastic plates, *Arch. Rat. Mech. Anal.* 67 (2) (1978) 111–149.

[3] S.S. Antman, Global properties of buckled states of plates that can suffer thickness changes, *Arch. Rat. Mech. Anal.* 110 (1990) 103–117.
[4] S.S. Antman and E.R. Carbone, Shear and necking instabilities in nonlinear elasticity, *J. Elasticity* 7 (1977) 125–151.
[5] F. Brezzi, J. Rappaz and P.A. Raviart, Finite dimensional approximation of nonlinear problems, Part I: Branches of nonsingular solutions, *Numer. Math.* 36 (1980) 1–25.
[6] F. Brezzi, J. Rappaz and P.A. Raviart, Finite dimensional approximation of nonlinear problems, Part II: Limit points, *Numer. Math.* 37 (1981) 1–28.
[7] F. Brezzi, J. Rappaz and P.A. Raviart, Finite dimensional approximation of nonlinear problems, Part III: Simple bifurcation points, *Numer. Math.* 38 (1981) 1–30.
[8] J. Carr, M. Gurtin and M. Slemrod, Structured phase transitions on a finite interval, *Arch. Rat. Mech. Anal.* 86 (1984) 317–351.
[9] J. Carr, M. Gurtin and M. Slemrod, One-dimensional structured phase transformations under prescribed loads, *J. Elasticity* 15 (1985) 133–142.
[10] M.G. Crandall and P.H. Rabinowitz, Nonlinear Sturm–Liouville problems and topological degree, *J. Math. Mech.* 19 (1970) 1083–1102.
[11] M.G. Crandall and P.H. Rabinowitz, Bifurcation from simple eigenvalues, *J. Functional Analysis* 8 (1971) 321–340.
[12] M.G. Crandall and P.H. Rabinowitz, Bifurcation, perturbation of simple eigenvalues and linearized stability, *Arch. Rat. Mech. Anal.* 52 (1973) 160–192.
[13] J.L. Ericksen, Equilibrium of bars, *J. Elasticity* 5 (1975) 191–201.
[14] T.J. Healey, Symmetry and nodal properties of systems of nonlinear Sturm–Liouville eigenvalue problems, Tech. Report, Department of Theoretical and Applied Mechanics and Center for Applied Mathematics, Cornell University, Ithaca, NY (1990).
[15] T.J. Healey and H. Kielhofer, Symmetry and nodal properties in global bifurcation analysis of quasilinear elliptic equations, *Arch. Rat. Mech. Anal.* 113 (1991) 299–311.
[16] T.J. Healey and H. Kielhofer, Hidden symmetries of fully nonlinear boundary conditions in elliptic equations: global bifurcation and nodal structure, *Results in Mathematics* 21 (1992) 83–92.
[17] J.H. Maddocks, Stability and folds, *Arch. Rat. Mech. Anal.* 99 (1987) 301–328.
[18] P.M. Naghdi, The theory of plates and shells, in: C. Truesdell, ed., *Handbuch der Physik, Vol. 2* (Springer, Berlin, 1972) 425–640.
[19] P.V. Negrón-Marrero, Necked states of non-linearly elastic plates, *Proc. Roy. Soc. Edinburgh* 112A (1989) 277–291.
[20] P.V. Negrón-Marrero and S.S. Antman, Singular global bifurcation problems for the buckling of anisotropic plates, *Proc. Roy. Soc. Lond.* A 427 (1990) 95–137.
[21] P.V. Negrón-Marrero and C. Carbonera, The numerical computation of compressed states of nonlinearly elastic anisotropic plates, *Numer. Math.* 56 (1989) 93–107.
[22] N. Owen, Existence and stability of necking deformations for nonlinearly elastic rods, *Arch. Rat. Mech. Anal.* 98 (1987) 357–383.
[23] W.C. Rheinboldt, Numerical methods for a class of finite dimensional bifurcation problems, *SIAM J. Numer. Anal.* 15 (1978) 1–11.
[24] W.C. Rheinboldt, *Numerical Analysis of Parametrized Nonlinear Equations* (Wiley, New York, 1986).
[25] D.H. Satinger, Stability of solutions of nonlinear equations, *J. Math. Anal. Appl.* 39 (1972) 1–12.
[26] K.-G. Shih and S.S. Antman, Qualitative properties of large buckled states of spherical shells, *Arch. Rat. Mech. Anal.* 93 (1986) 357–384.
[27] B. Smith, J. Boyle, J. Dongarra, B. Garbow, Y. Ikebe, V. Klema and C. Moler, *Matrix Eigensystem Routines — EISPACK Guide*, Lecture Notes in Computer Science (Springer, New York, 2nd ed., 1976).
[28] H. Weinberger, On the stability of bifurcating solutions, Reprint from: *Nonlinear Analysis* (dedicated to Erich Rothe) (Academic Press, New York, 1978).